

Quantifying coconut palm extent on Pacific islands using spectral and textural analysis of very high resolution imagery

Michael W. Burnett, Timothy D. White, Douglas J. McCauley, Giulio A. De Leo & Fiorenza Micheli

To cite this article: Michael W. Burnett, Timothy D. White, Douglas J. McCauley, Giulio A. De Leo & Fiorenza Micheli (2019): Quantifying coconut palm extent on Pacific islands using spectral and textural analysis of very high resolution imagery, International Journal of Remote Sensing, DOI: [10.1080/01431161.2019.1594440](https://doi.org/10.1080/01431161.2019.1594440)

To link to this article: <https://doi.org/10.1080/01431161.2019.1594440>



Published online: 28 Mar 2019.



Submit your article to this journal [↗](#)






Article views: 64



View Crossmark data [↗](#)



Quantifying coconut palm extent on Pacific islands using spectral and textural analysis of very high resolution imagery

Michael W. Burnett^a, Timothy D. White^b, Douglas J. McCauley ^{c,d},
Giulio A. De Leo ^b and Fiorenza Micheli ^{b,e}

^aEarth Systems Program, Stanford University, Stanford, CA, USA; ^bHopkins Marine Station, Stanford University, Pacific Grove, CA, USA; ^cDepartment of Ecology, Evolution, and Marine Biology, University of California Santa Barbara, Santa Barbara, CA, USA; ^dMarine Science Institute, University of California Santa Barbara, Santa Barbara, CA, USA; ^eCenter for Ocean Solutions, Stanford University, Pacific Grove, CA, USA

ABSTRACT

Native forests on islands throughout the global tropics face increasing pressure from the human-driven expansion of coconut palm (*Cocos nucifera*) planted for the purposes of coconut oil harvest. Conversion from native forests to *Cocos* monocultures leads to drastic ecological consequences in island environments and alters terrestrial and marine food webs through a variety of cascading effects and feedbacks. Despite the ecological significance and geographic range of *Cocos* expansion, large-scale assessments of coconut proliferation are still lacking due to the isolated nature of many islands where *Cocos* is found. Remote sensing approaches are often used to monitor forest composition at broad scales, but the small physical size of most islands limits the use of many popular satellite sensors with 15–30 m resolution. The recent availability of very high resolution (<5 m) satellite imagery facilitates novel assessment of this major ecological pattern, but the increased resolution introduces problematic ‘salt-and-pepper’ effects due to the heterogeneous nature of palm frond canopies. This case study evaluates the effectiveness of applying grey-level co-occurrence matrix (GLCM) textural features to very high resolution (0.5–2 m) WorldView-2 imagery to resolve the canopy heterogeneity problem and map the extent of *Cocos* spread on 21 islets of Palmyra Atoll, a protected United States National Wildlife Refuge in the Northern Line Islands. A random forest (RF)-driven classification scheme differentiating between coconut palms, native trees including *Pisonia grandis*, and endemic *Scaevola sericea* shrubs achieved 97.0% overall accuracy and 98.4% producer’s and user’s accuracies for the coconut palm class when trained on a combined spectral and GLCM textural feature set. Classifications restricted to the eight spectral bands of WorldView-2 are not only less accurate (89.4% overall accuracy), but also significantly worse at identifying *Cocos* canopies (79.0% versus 98.0% accuracy when GLCM textures are included). However, paring down the full set of sixteen spectral and textural features to the three most important of each type did not result in significant changes in accuracy. These results demonstrate the effectiveness of a joint high-resolution textural and spectral approach for remotely quantifying the spread of *Cocos* and its impacts on native tree communities throughout the tropics, including remote island locations.

ARTICLE HISTORY

Received 26 February 2019
Accepted 3 March 2019

1. Introduction

Native forests throughout the tropics face increasing pressure from anthropogenic land use changes, climate change, and invasive species (Seddon et al. 2016; Hansen et al. 2013; Fine 2002). Native species on tropical islands are especially vulnerable to anthropogenic impacts due to their geographic isolation and the typically small size of their island habitats (Fordham and Brook 2010). Native plant communities have been cleared on many tropical Indo-Pacific islands in favour of coconut palm plantations (Mueller-Dombois and Fosberg 1998), which often provide a primary means of economic gain and subsistence in isolated island environments (Vergara and Nair 1985). The conversion of native island forests, often characterized by broadleaf trees including *Pisonia grandis* and *Tournefortia argentea*, to *Cocos* monocultures leads to drastic ecological consequences for atoll ecosystems. For instance, island flora may face increased competition for freshwater (Krauss et al. 2015), nutrient depletion (Young et al. 2010), and increased seedling damage from litterfall (Young et al. 2014). Increasingly rare native *Pisonia* forests also provide critical habitat for insects (Handler et al. 2007), reptiles (Briggs et al. 2012), and seabird colonies (Kepler and Kepler 1994; Walker 1991), which help create important phosphate soils that support many plant species on otherwise nutrient-poor parent material (Fosberg 1957). Through a complex network of land-sea interactions, *Cocos* invasions and the loss of native forests can profoundly alter not only terrestrial ecosystems but also marine food webs (Young et al. 2017; McCauley et al. 2012).

While there is scattered documentation of *Cocos* proliferation in individual locations (Mueller-Dombois and Fosberg 1998), a systematic, broader-scale assessment of the intrusion of coconut palms into tropical island forests is needed to evaluate the magnitude and status of this widespread conservation issue – a difficult task given the isolation and abundance of affected islands. Remote sensing techniques have been used in similar forestry applications with much success (Huang and Asner 2009), and some studies have developed methodologies to remotely map actively-managed palm plantations in regions of tropical forest using their organized spatial arrangements (e.g. Komba Mayossa et al. 2015; Koh et al. 2011). However, the satellite sensors most commonly used for land cover studies typically feature 10 to 30-meter spatial resolutions, which are too coarse to examine biological invasions in the heterogeneous terrestrial environments found on the narrow land areas of most atolls. For instance, the widest section of the vegetated rim of Palmyra Atoll, one of the Northern Line Islands in the Pacific Ocean and the basis of this case study, is less than 450 m across. Very high resolution (<5 m) satellite sensors have launched in growing numbers over the past two decades, but they introduce spatial heterogeneity within forest types that make pixel-based classification difficult – also known as the ‘salt-and-pepper effect’ (Yu et al. 2006). When viewed through high-resolution datasets, land cover types often exhibit visual heterogeneity that can confuse classification algorithms searching for a land cover type’s distinct spectral signature. While low resolution sensors effectively smooth out this variability, high resolution sensors inherently capture pixels with more or less brightness than their neighbours within the same class (e.g. a palm frond pixel with higher brightness than an adjacent shadowed pixel), hence the salt-and-pepper analogy. For these reasons, few atolls’ terrestrial ecosystems have been analysed via remote sensing, and large-scale estimates of tropical island forest change are lacking.

The present study applies a combination of remote sensing techniques to overcome these limitations and quantify the extent of *Cocos* and native forest habitats on a tropical atoll. Specifically, we used very high resolution (0.5–2 m) multispectral data to capture the small-scale spatial variability of the atoll's vegetation, and grey-level co-occurrence matrix (GLCM) textural analysis – a statistical approach to examine texture based on the value and spatial relationship of pixels – to leverage the high spatial heterogeneity of *Cocos* tree canopies to classify forest types. Recent studies have applied very high resolution remote sensing data and GLCM analysis to land cover classification problems with much success (Kaszta et al. 2016; Wang et al. 2016; Bricher et al. 2013; Murray, Lucieer, and Williams 2010). Here, we apply this combination to an understudied tropical island terrestrial ecosystem and then use a random forest (RF) algorithm to map the distribution of *Cocos* and native trees. Random forest algorithms have seen growing popularity in land cover classification studies due to their strong performance relative to other classification algorithms (Le Louarn et al. 2017; Ma et al. 2017; Kaszta et al. 2016; Shiraishi et al. 2014; Cutler et al. 2007) and their low sensitivity to problems like noisy data and over-training on large forests (Rodriguez-Galiano et al. 2012a). Using Palmyra Atoll, a remote US atoll located in the central Pacific Ocean, as a case study, we demonstrate our approach's ability to remotely map *Cocos* trees and native forests with very high accuracy even in isolated and small island ecosystems.

2. Methods

2.1. Study area

Palmyra Atoll, a United States National Wildlife Refuge, is located in the central Pacific Ocean at 05°53' N, 162°05' W, 1,700 km southwest of Hawai'i. While the geomorphology of the atoll was extensively altered to accommodate a US military base from 1940 to 1945 (Collen, Garton, and Gardner 2009), subsequent private ownership and Palmyra's eventual designation as a National Wildlife Refuge in 2001 have allowed for the establishment of an extensive forest ecosystem on the atoll (McCauley et al. 2012). Classified as a wet atoll (rainfall > 4,000 mm/yr) (Mueller-Dombois and Fosberg 1998) with a coral-sand composition and some freshwater retention in its belowground system (Hathaway, McEachern, and Fisher 2011), Palmyra hosts some of the region's largest tracts of native broadleaf trees (*P. grandis*, *T. argentea*, etc.) in addition to *Cocos nucifera* (Krauss et al. 2015). Today, Palmyra's uninhabited islets are dominated by two main forest types: forests primarily composed of tall *P. grandis* trees with fringing *T. argentea*, and forests consisting almost completely of *Cocos* monoculture, with different degrees of mixing between those two forest types (Young et al. 2010; Wester 1985). Additionally, some areas of the atoll contain dense growths of the native shrub *Scaevola sericea* and the non-native tree *Terminalia catappa* (Lafferty et al. 2010; Wegmann 2005). The native monocot screw pine *Pandanus tectorius* is also present in small stands on Palmyra. As Palmyra's protected forests contain many of the major tree species found throughout the Indo-Pacific, Palmyra presents an excellent case study for the remote detection of *Cocos* versus native broadleaf forests.

Humans drastically increased the abundance and range of *Cocos* on Palmyra Atoll in the 19th and 20th centuries, though the earliest history of *Cocos* on Palmyra is uncertain (Young et al. 2010; Wegmann 2009). As occurred on many other Indo-Pacific atolls,

extensive native forests were cleared for military operations and commercial *Cocos* plantations, which were active on Palmyra as recently as the 1970s (Hathaway, McEachern, and Fisher 2011; Young et al. 2010; Krauss 1979; Dawson 1959; Rock 1916). In this study, the term 'native forest' refers to the prevalent non-*Cocos* native tree species (namely *P. grandis* and *T. argentea*) that frequently compete with *Cocos* for space and resources on small islands.

Fieldwork was conducted over several weeks during June and July of 2017. We collected ground-validated points representing our three primary vegetation cover types: (A) native forest, mostly consisting of broadleaf trees *P. grandis* and *T. argentea*; (B) *Cocos*-dominated forest; and (C) *Scaevola* shrubs (see Figure 1). These three classes are by far the dominant vegetation types present on the atoll, and combined represent nearly its entire land area (Wegmann 2005). Because of *T. catappa*'s absence on most islets and its structural similarities to *P. grandis*, it was included in the native forest class of our analysis despite being non-native to Palmyra. The tree is only present on one of the atoll's islets and does not pose the conservation risk that *Cocos* does throughout the region. The monocot *P. tectorius*, which is present in small stands intermixed with other vegetation types, was not abundant enough to warrant its own class and is instead included in the native forest class alongside the larger broadleaf tree species.

2.2. Remote sensing data

A WorldView-2 2A-level multispectral image of Palmyra Atoll was provided by the DigitalGlobe Foundation (see Figure 1). The image was taken on 20 December 2016, and consists of eight multispectral bands with a 2-meter spatial resolution, as well as a panchromatic band with 0.5-meter resolution (see Table 1). The selected image was chosen because it is fairly recent and almost completely cloudless. The image was radiometrically and geometrically corrected with a coarse terrain elevation model; given the flat nature of the atoll, this correction is likely sufficient to overcome terrain effects. The data were atmospherically corrected using DigitalGlobe's proprietary Atmospheric Compensation (AComp) process, which has proven very effective in tropical settings with high levels of atmospheric water vapor (Cross et al. 2018; Pacifici 2016; Smith 2015).

Before calculating textural features and growing the random forest, the eight multispectral bands were down-scaled from 2-meter pixels to 0.5-meter pixels using QGIS 3.0.0 software (QGIS Development Team 2009). As the panchromatic and multispectral pixels are all perfectly aligned, no statistical resampling or panchromatic sharpening (pansharpening) of the multispectral data was necessary – the 2-meter pixels were simply divided into sixteen smaller pixels with a conserved value in order to produce a classification with 0.5-meter pixels. This approach allowed us to grow our random forest with the greatest possible amount of textural information (contained within the 0.5-meter panchromatic band) without introducing the added uncertainties of pansharpening the multispectral data (Li, Jing, and Tang 2017).

2.3. Grey-level co-occurrence matrix (GLCM) textural features

Texture analysis is an important tool for remotely classifying land cover types with low inter-class variability or a large amount of intra-class heterogeneity (Myint, Lam, and



Figure 1. WorldView-2 image of Palmyra Atoll (December 2016) with aerial and ground-level views of: (a) native broadleaf forest; (b) *Cocos*-dominated forest; and (c) *Scaevola* shrub thicket. Satellite images courtesy of the DigitalGlobe Foundation.

Table 1. WorldView-2's eight multispectral bands and the eight GLCM textural features calculated from the panchromatic band.

Feature	Spectral Band	Wavelengths (nm)
B1	Coastal	400–450
B2	Blue	450–510
B3	Green	510–580
B4	Yellow	585–625
B5	Red	630–690
B6	Red-edge	705–745
B7	Near-IR 1	770–895
B8	Near-IR 2	860–1040
Feature	GLCM Texture (pan)	Texture Group (Hall-Beyer 2017b)
T1	Mean	Statistical
T2	Variance	Statistical
T3	Homogeneity	Contrast
T4	Contrast	Contrast
T5	Dissimilarity	Contrast
T6	Entropy	Orderliness
T7	Second Moment	Orderliness
T8	Correlation	Statistical

Tyler 2004; Irons and Petersen 1981). In particular, the grey-level co-occurrence matrix (GLCM) (Haralick, Shanmugan, and Dinstein 1973) is a widely-used method for extracting textural features from remote sensing data (Hall-Beyer 2017a; Marceau et al. 1990). While the GLCM features may be extracted from many combinations of multispectral bands and their principal components, most studies choose to simply use one spectral band or a panchromatic band, if available (Hall-Beyer 2017a; Huang, Liu, and Zhang 2014). Exclusive use of the panchromatic band for generating GLCM features may result in some loss of information (Huang, Liu, and Zhang 2014), but many studies still achieve significant increases in classification accuracy at reduced computational cost by restricting GLCM calculation to a single band (Pacifci, Chini, and Emery 2009; Puissant, Hirscha, and Webera 2005). Given the very high spatial resolution of WorldView-2's panchromatic band (0.5 meters) and the easily differentiable canopy 'textures' of Cocos and native broadleaf trees, we elected to extract our GLCM features directly from the panchromatic band.

GLCM features were calculated using the 'glcm' and 'raster' packages (Zvoleff 2016; Hijmans 2017) for R software, version 3.2.2 (R Core Team 2016). Eight textural features reported in Table 1 were calculated for a range of window sizes, from 3-by-3 pixel squares to 30-by-30 pixel squares (Hall-Beyer 2017b). For all of these window sizes, the central pixel is classified using textural information extracted from across the entire window (Hall-Beyer 2017b). By visually examining the resulting texture maps (see Figure 2), we found that a 17-by-17 pixel square window produced the greatest average difference between Cocos and native broadleaf canopies while still preserving class edges (Murray, Lucieer, and Williams 2010). Given our 0.5-meter resampled resolution, this window corresponds to a square with 8.5 meter sides – slightly longer than a mature coconut palm frond (Young et al. 2014). A larger window size allows the classifier to draw on more texture information when

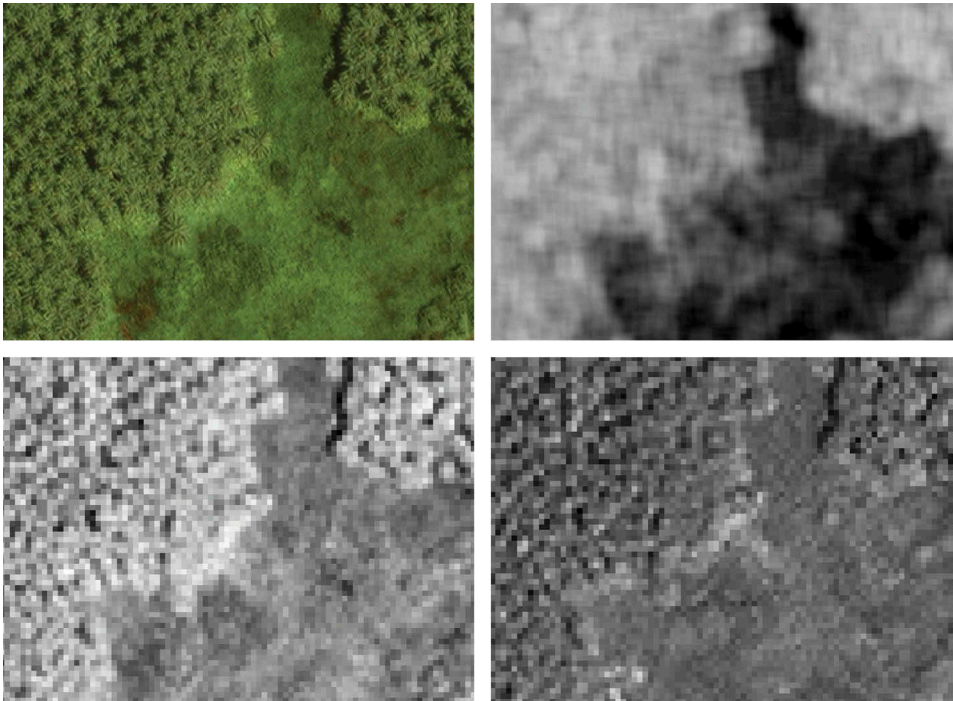


Figure 2. Clockwise from upper-left panel: (a) pansharpened WV-2 imagery showing a mix of *Cocos* and *Scaevola* thickets on Cooper Island, Palmyra Atoll; (b) GLCM entropy (T6) calculated with a 17-by-17 pixel window over the same area; (c) singleband rendering of the WV-2 red band (B5) over the same area; and (d) singleband rendering of the WV-2 NIR-1 band (B7). Note that while general differences between the two land cover types are visible in the WV-2 spectral data, the data also contain significant variability within each class (the so-called ‘salt-and-pepper effect’) that can be captured well by texture measures like GLCM entropy. Satellite images courtesy of the DigitalGlobe Foundation.

evaluating a given pixel, which could increase accuracy; however, enlarging the scope of the GLCM window will reduce sensitivity to land cover class edges (Clausi 2002) and effectively smooth over the image. As our 17-by-17 pixel window is large enough to encompass whole palm fronds (and the shadows around them) but is spatially smaller than the GLCM windows of other very high resolution land cover classification studies (Kaszta et al. 2016; Wang et al. 2016; Bricher et al. 2013), we conclude that it is appropriate for capturing both intra-class textural qualities and inter-class edges within our study system.

Hall-Beyer (2017a) notes that many of the GLCM measures are highly correlated with one another. If these correlated features are used as input variables for the classifier algorithm, classification accuracy could be reduced due to the imbalanced weighting of the largest correlated feature groups (Murray, Lucieer, and Williams 2010; Pacifici, Chini, and Emery 2009). The eight measures implemented in this study may be categorized into the three uncorrelated groups found in Table 1: mean, variance, and correlation are essentially ‘descriptive statistics;’ homogeneity, contrast, and dissimilarity are ‘contrast’-based; and entropy and second moment are measures of ‘orderliness’ (Hall-Beyer 2017b). Following previous GLCM-based modeling efforts (Ozdemir and Karnieli 2011;

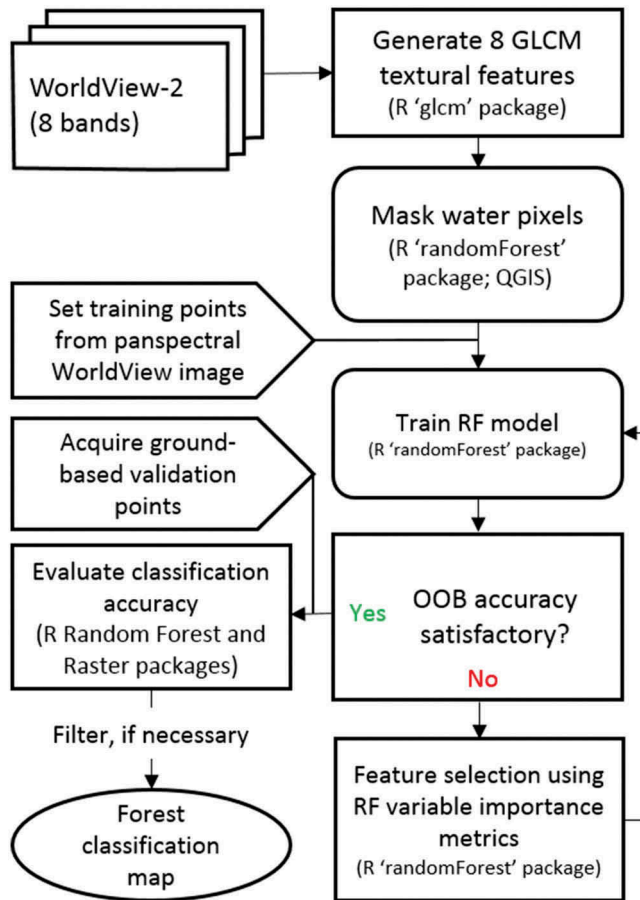


Figure 3. Workflow figure for generating the final classification map. Software packages used are specified for most steps; both R and QGIS are available as free, open-source programs (R Core Team 2016; QGIS Development Team 2009).

Murray, Lucieer, and Williams 2010), we chose the most influential texture feature from each of the three uncorrelated categories as described in Table 1 (Hall-Beyer 2017b). This ‘feature selection’ step (see Figure 3) is described in detail in Section 2.5.2.

2.4. Validation and training data

The RF classifier was trained on 800 geographic points acquired directly from our WorldView-2 image. Previous RF classification studies have observed overall accuracy plateaus once the number of training pixels per class exceeds about 3–7 times the number of training features (Millard and Richardson 2015; Rodriguez-Galiano et al. 2012b; Pal and Mather 2003). However, such results are specific to their exact study situations and to the levels of intra-class variability present (Rodriguez-Galiano et al. 2012b). Others have broadly recommended using at least 10 times as many training pixels per class as total features in decision tree-based classifications (Pal and Mather

2003). Following this recommendation, we selected 200 training points per class (12.5 times the 16 possible features used in this study) on which to grow our RF model.

To prevent biased training data, we implemented a stratified random sampling design in which polygons were drawn around areas of clearly homogenous vegetation type throughout the atoll ring and a random subset of pixels was selected from within each polygon (Stehman 2009), sampling both areas near class edges and areas near the centers of homogenous polygons. The inclusion of pixels near class edges meant the RF model would be trained in locations where some portion of the GLCM window overlapped other land cover types as well – an important consideration for improving the classifier’s edge detection. Our vegetation classes and non-vegetated areas are easily distinguished using WorldView-2’s very high resolution imagery (see Figure 1) combined with firsthand knowledge of Palmyra Atoll’s vegetation and the previous mapping efforts of Wegmann (2005). We collected an equal number of points for each of our four classes because the accuracy of a random forest model may decrease when training from imbalanced data (Chen, Liaw, and Breiman 2004). For each point, we extracted the values of the 8 spectral bands and the 8 GLCM texture features in the process of training the RF classifier, as described in section 2.5.

During the month of July 2017, we collected a total of 496 ground-sampled validation points on Palmyra Atoll that represent our four land cover classes (see Table 2). These points were used to independently cross-validate our classification results and produce overall accuracy statistics, as they were held out of the training process. To create this validation dataset, a simple random sample of 600 points was generated over the land area of Palmyra Atoll. Each accessible point was visited and its canopy type logged; in addition, each point was verified to represent homogenous canopy cover over a ~ 10-meter radius around the point in order to account for the accuracy of the handheld GPS receiver. Any point that failed this condition or proved inaccessible due to wildlife-related restrictions was removed, ultimately resulting in 496 validation points. Even after the removal of all points from several small islets that proved inaccessible, the sampled area still represents at least 90% of the atoll’s land area, ensuring any variability within classes across the atoll is captured. In several cases of random points landing on narrow non-vegetated features like roads and beaches (where land cover boundaries are more clearly visible than between two vegetated classes), the points were visually inspected over the WorldView-2 image after ground-validation to ensure accurate class designations.

2.5. Random forest (RF) classification

We classified the entire terrestrial portion of the WorldView-2 image using a random forest (RF) model, as implemented in the ‘randomForest’ package (Liaw and Wiener 2002) in R (R Core Team 2016). RF models are bootstrapped ensembles of many classification trees that

Table 2. Number of training and validation points for each land cover class.

Land Cover Class	Training Points	Validation Points
Coconut palm	200	187
Native forest	200	191
<i>Scaevola sericea</i> shrub	200	57
Non-vegetation	200	61

can handle many independent variables while providing very high accuracy (Shiraishi et al. 2014; Evans and Cushman 2009; Breiman 2001). Each tree also implements a randomized bagging approach to remove a subset of training data and use it to cross-validate the result of each tree, allowing RF to provide a built-in ‘out-of-bag’ (OOB) accuracy as well as metrics of input feature importance (Pal 2005; Breiman 2001).

The RF model was constructed using a pixel-based approach: individual training pixels are used to train the algorithm, and the algorithm subsequently classifies every pixel in the image. Many forest classification studies alternatively use object-based approaches to great effect (e.g. Immitzer, Atzberger, and Koukal 2012; Yu et al. 2006), including recent efforts to detect and count individual oil palms in spatially-organized plantations (Li et al. 2016). But because Palmyra Atoll features dense forests with complex, intermixed tree crowns and no maintained spatial arrangement, object-based classification approaches were not included in this study to eliminate potential errors in the segmentation process (Liu and Xia 2010).

We use 800 remotely-acquired training points to grow an RF using all sixteen available features (see Table 1), which provides the statistical associations necessary to conduct further feature selection to the three most influential uncorrelated textural and spectral features. Then, a new RF grown off the pared-down feature set is used to classify the entire 2016 WorldView-2 image. The accuracy of the resulting classification map is evaluated using the 496 validation points described above, while OOB accuracy estimates are used to compare this feature-selected RF classification to those produced using only spectral features, only textural features, and the entire set of sixteen combined features. These processes are described in depth below.

2.5.1. Water masking

Before classifying the image, water pixels were masked by growing an RF model using only WorldView-2's NIR-1 and NIR-2 bands and two classes: land and water. Land pixels were trained with the aforementioned 800 training points; water pixels were trained on a set of 400 new points chosen from the deep ocean, lagoon, and reef shallows around Palmyra. Since water has very low reflectivity in the near-IR spectral range (Bartolucci, Robinson, and Silva 1977), this simple random forest model was able to accurately classify the entire image as either land or water. In addition, we manually removed several misclassified instances of breaking waves, which can exhibit an abnormally high NIR reflectance due to added surface roughness (Gordon and Wang 1992). While a simple RF model could be built with the same binary approach to detect all vegetation and mask out all non-vegetated land alongside water pixels, we were interested in measuring the total land area of Palmyra and its islets and therefore designated non-vegetated land as its own class within the main RF classifier.

2.5.2. Feature selection

First, the masked WorldView-2 image was classified using an RF model grown from all sixteen features. However, previous work shows that correlation between independent variables can adversely impact RF classification accuracy, even despite RF's robust bagging approach (Gregorutti, Michel, and Saint-Pierre 2017; Boulesteix et al. 2012; Pacifici, Chini, and Emery 2009). We addressed this by dividing the eight spectral bands of WorldView-2 into three mostly-uncorrelated categories: the Coastal and Blue bands (B1-

B2); the Green, Yellow, and Red bands (B3-B5); and the Red-edge, NIR-1, and NIR-2 bands (B6-B8) (Immitzer, Atzberger, and Koukal 2012). In essence this approach is very similar to our selection of the three best uncorrelated GLCM features – it allows the user to efficiently select an optimal feature set using the standard RF-generated variable importance plots. We then selected the most influential features in each spectral or textural category using the variable importance indices generated by the sixteen-feature RF model (see Figure 4). The first index, Mean Decrease in Accuracy (MDA), uses RF's constantly-permuting OOB samples to find the added error rate associated with any given input variable's exclusion from a tree (Genuer, Poggi, and Tuleau-Malot 2010). The second index, Mean Decrease in Gini (MDG), measures the forest-wide average decrease in node impurities from splits on a given variable, as measured by the Gini index (Han, Guo, and Yu 2016). In both cases, the larger the index, the more influential was the corresponding variable. Han, Guo, and Yu (2016) suggest a combined ranking of MDA and MDG as a robust feature selection procedure; we calculate this variable importance score by averaging a variable's ranks in the MDA and MDG plots (see Figure 4).

Using our combined ranking (see Figure 4) and the feature categories established above, we selected the Correlation (T8), Dissimilarity (T5), and Entropy (T6) GLCM measures and the Coastal (B1), Red (B5), and NIR-1 (B7) spectral bands. Our three GLCM choices agree well with Hall-Beyer (2017b), which proposes that classification studies in which a class patch might contain 'edge-like features' (like coconut palm fronds) should consider Correlation over Mean and Variance, Dissimilarity or Contrast over Homogeneity, and Entropy over Second Moment. See Hall-Beyer (2017a) for descriptions of each GLCM measure.

2.5.3. Modal filtering

Finally, the resulting classification was smoothed with a 5-by-5 pixel modal (majority) filter (Booth and Oldfield 1989). This step was integrated into the end of the

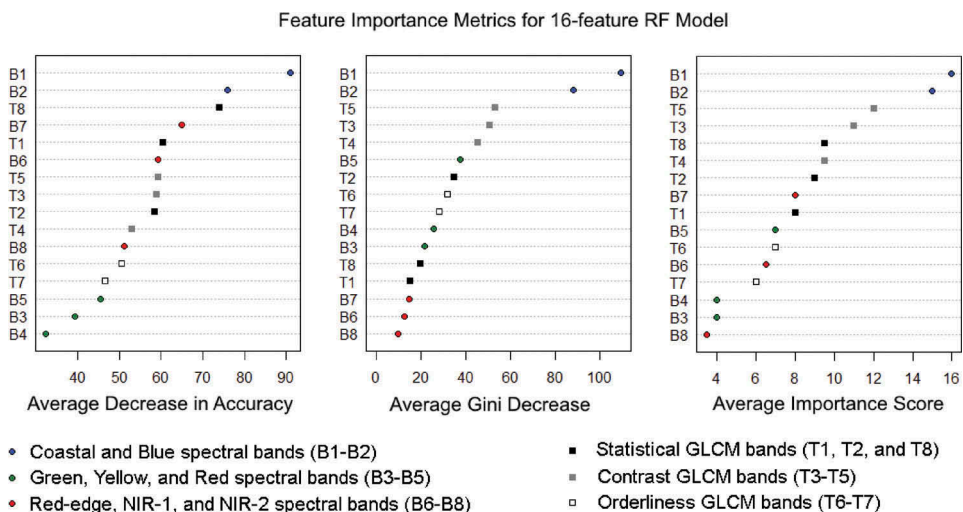


Figure 4. Feature importance metrics derived from the randomForest R package (Liaw and Wiener 2002) for the 16-band RF model. The right pane presents the averaged MDA and MDG rankings of each feature, with a higher score representing greater variable importance.

classification workflow (see [Figure 3](#)) to remove remaining salt-and-pepper noise, eliminate outlier pixel classifications that are likely too small to represent a true signal in the forest canopy, and facilitate map interpretation. Since each pixel in the final classification is 0.5-by-0.5 m, the 5-by-5 modal filter evaluated each pixel within the context of its neighbors 1 m in any direction. As it is unlikely that a tree crown with a visible diameter of <1 m could be reliably detected within Palmyra's mature forest canopy, the filter removed such isolated pixel clusters if their context contained another more dominant vegetation class.

3. Results

The total land area estimated by classifying the entire water-masked image of Palmyra (see [Figure 5](#)) is 2.37 square kilometres – very close to a manually-derived land area estimate of 2.46 km² for the year 2000, especially when considering tidal differences and the dynamic nature of sandy islets (Collen, Garton, and Gardner 2009). Of Palmyra's 2.37 km² land area, we find that *Cocos* canopies occupy 1.00 km² (42.3%), native forest tree canopies cover 0.79 km² (33.4%), and *S. sericea* shrubs cover 0.19 km² (8.2%). The remaining land area (0.38 km²; 16.1%) is classified as non-vegetated, and includes buildings, roads, an airstrip, mowed grass (maintained by field station personnel and resistant to colonization by other vegetation types), and sand. The mix of land cover is highly variable from islet to islet (see [Figure 5](#)): for instance, Sand Island – the southwestern islet in the atoll ring – is 81.7% native forest and 12.3% *Cocos*. On the other hand, the southern portion of the atoll ring is 6.2% native forest, 76.1% *Cocos*, and 17.6% non-vegetated. See Appendix A for land cover information of each of Palmyra's islets and this article's online supplemental materials for the full-sized, georeferenced classification file.

The feature-selected model's overall out-of-bag (OOB) error stabilized at 4.6% after running approximately 2,000 trees (see [Figure 6](#)), but in case variable interaction stabilizes at a slower rate than OOB error, our forest size was expanded to 6,000 trees (Evans and Cushman 2009). Native forest exhibited the greatest OOB error with 8.0%, while *Cocos* and non-vegetation tied for the low OOB error of 2.5%. The spectral-only and textural-only models have trouble detecting different classes – as expected, the spectral model (10.6% OOB error) struggles to correctly classify *Cocos* while easily

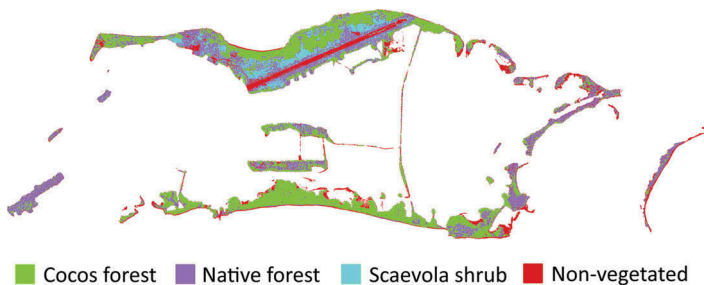


Figure 5. The completed RF classification of Palmyra using the six selected features and a 5-by-5 pixel modal filter. The full-resolution, georeferenced classification map of Palmyra Atoll's vegetation can be downloaded from the Open Science Framework at <https://osf.io/j2sta/> (doi:10.17605/OSF.IO/J2STA).

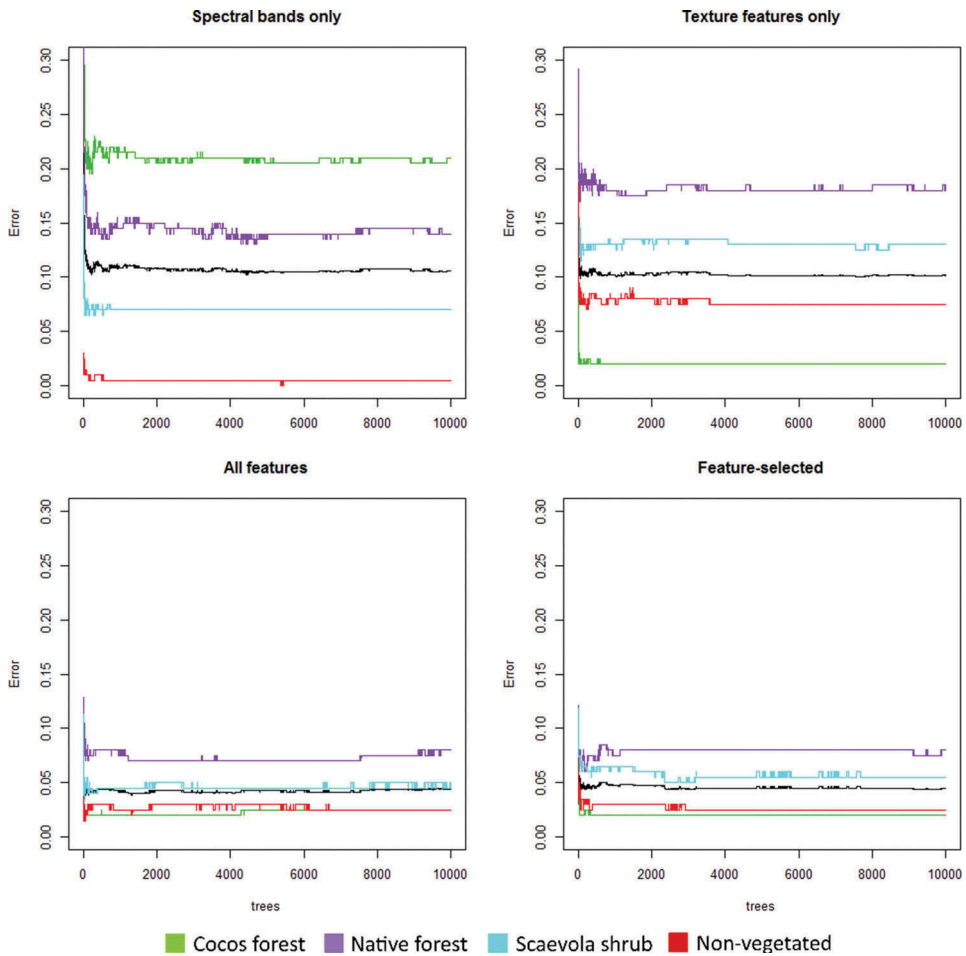


Figure 6. Out-of-bag errors for each land cover class (see legend) and the RF models overall (black line) versus the number of decision trees grown in the forest (plotted here up to 10,000 trees). Upper left: an RF model trained on only spectral bands. Upper right: an RF model trained on only textural bands. Lower left: an RF model trained on all sixteen features. Lower right: an RF model trained on three selected spectral bands and three selected GLCM textural measures.

identifying nearly all non-vegetated pixels; on the other hand, the textural model (10.1% OOB error) finds *Cocos* canopy the most easily identifiable while error rates increase for the other three classes. Combining spectral and textural features decreased OOB error significantly, as seen in both the sixteen-feature model and the feature-selected model. However, the feature-selected model achieved very similar results to the sixteen-band model, suggesting the feature reduction step may be unnecessary in this instance.

In addition to the OOB error provided by the RF model based on 800 training points, we use cross-validation with our 496 ground-collected points to determine our classification's accuracy (see Table 3). Overall classification accuracy equaled 95.4% using OOB estimation and 97.0% using cross-validation.

In order to evaluate the performance of the RF classification for each specific land cover class, we provide producer's and user's accuracies calculated with both OOB

Table 3. Top: Confusion matrix derived from the feature-selected RF model's OOB errors for the 800 training points. Bottom: Confusion matrix calculated by cross-validating the smoothed, feature-selected RF classification against 496 validation points. Columns represent the true vegetation types at training or validation points while rows represent the classification results at those points.

Classified as:	Coconut palm	Native forest	<i>Scaevola</i> shrub	Non-vegetation	Producer's Accuracy	User's Accuracy
Out-of-bag accuracy statistics						
Coconut palm	196	3	1	0	0.961	0.980
Native forest	5	184	9	2	0.920	0.920
<i>Scaevola</i> shrub	0	12	188	0	0.945	0.940
Non-veg.	3	1	1	195	0.990	0.975
Overall OOB accuracy:						0.954
Cross-validated accuracy statistics						
Coconut palm	184	3	0	0	0.984	0.984
Native forest	0	183	2	2	0.958	0.979
<i>Scaevola</i> shrub	3	4	55	0	0.965	0.887
Non-veg.	0	1	0	59	0.967	0.983
Overall validated accuracy:						0.970

(applied to 800 training points) and cross-validated (applied to 496 validation points) statistics in Table 3. Producer's accuracy can be likened to precision for an individual class; it represents the likelihood that real features on the ground are correctly represented in the classification (Pratomo et al. 2017). User's accuracy, similar to recall, is the likelihood that features shown in the classification map are actually present in reality (Pratomo et al. 2017). Cross-validation found *Scaevola sericea* shrubs to have the lowest user's accuracy at 88.7%, meaning 11.3% of pixels classified as *Scaevola* represent another vegetation type in reality. However, the cross-validated producer's accuracy of *Scaevola* shrub was much greater at 96.5%, indicating pixels that truly represent *Scaevola* were very frequently classified as such. The rest of the user's accuracies determined by cross-validation were all very high (>97.9%), and producer's accuracies for all classes exceeded 95%.

4. Discussion

4.1. Combined spectral and textural analysis

Tracking the changing distribution of introduced Cocos palms and the resulting decline of native tree species is crucial for effective management of tropical island ecosystems. Management communities across the Pacific have already undertaken efforts to actively remove Cocos stands in island systems in order to preserve native forests and their associated ecosystem benefits (e.g. Hathaway, McEachern, and Fisher 2011), but broad-scale assessments of the coconut palm's proliferation in these remote locations are lacking. Our results demonstrate that a combination of remote sensing techniques are very likely to assist in monitoring these vegetation classes on small, remote islands: using a combination of very high resolution imagery, GLCM textural analysis, and an RF classifier, an overall cross-

validated accuracy of 97.0% is achieved for a four-class classification of our study site. Such high accuracies are critical for assessing forest types on island environments, where even small intrusions of invasive species can significantly alter ecosystem function and eventually overtake entire islands (Young et al. 2017).

The combination of methods employed here proves essential for monitoring tropical island vegetation. Out-of-bag error estimates (see [Figure 6](#)) reveal that RF models trained exclusively on the eight spectral bands of WorldView-2 are less accurate overall than our feature-selected model (89.4% versus 95.4% OOB accuracy) and substantially worse at identifying *Cocos* canopies (79.0% versus 98.0% OOB accuracy), the primary target of this study. Prior studies have demonstrated that, even after atmospheric corrections are applied, the coastal (B1) and blue (B2) spectral bands are susceptible to significant attenuation by water vapour in the tropics that can render their data noisy or biased (Cross et al. 2018). To ensure these bands were not having an outsized negative effect on the spectral-only classification, the spectral RF model was re-grown without B1 and B2 to ultimately produce an overall OOB accuracy of 82.1%, with lower OOB accuracies for all four classes. Similar reductions in accuracy were seen when excluding B1 from the feature-selected model (91.9% overall OOB accuracy), with much greater confusion between the *Scaevola* and native forest classes. The reduced accuracy of both models after removing the coastal and blue spectral bands indicates that even in the humid tropics, both bands may retain a strong enough signal to help differentiate between broad vegetation classes after atmospheric corrections. Even so, users should apply these spectral bands cautiously when working in tropical environments, especially when more precise identification of vegetation is necessary or in contexts with a greater number of unique vegetation classes (Cross et al. 2018).

RF models grown using only the eight GLCM textural features are very effective at identifying *Cocos* (98.0% OOB accuracy), but achieve similar overall accuracy (89.9% OOB accuracy) to the spectral-only RF model. Accuracy appeared to suffer most in the texture-only RF model when classifying narrow features and class edges. While the models grown solely on spectral or textural data still show relatively high accuracies, the small number of classes in this classification and the objective of mapping trees to the scale of individuals set a very high bar for classification accuracy that is only properly met by the combined spectral-textural RF models.

Previously reported findings of spectral similarity between *Cocos* canopies and other island vegetation (Komba Mayossa et al. 2015; Lelong et al. 2004) are consistent with the above results. When this spectral confusion is paired with the salt-and-pepper problems inherent to the use of sub-meter imagery, textural analysis of the tree canopies becomes a necessary component of the classification process. By implementing GLCM textures in addition to multispectral data when training the RF classifier, we are able to produce a classification map with very high accuracy for all vegetation classes.

Palm tree detection proves an excellent demonstration of the combination's potential: previous studies have used satellite-based optical remote sensing to map oil palm agrosystems in tropical regions, but these efforts typically rely upon the open spatial arrangement of managed plantations to classify the palms (Lee et al. 2016; Li et al. 2016; Srestasathiern and Rakwatin 2014; Carlson et al. 2013; Koh et al. 2011; Thenkabail et al. 2004). Even efforts to map *Cocos* in Vanuatu in the South Pacific have likewise relied on open-canopy *Cocos* plantations for their segmentation and textural analyses (Komba

Mayossa et al. 2015; Lelong et al. 2004). These methods are unsuitable in the most common case of unmanaged Cocos plantations and in areas where former plantation efforts have established runaway Cocos forests, as on Palmyra Atoll (Young et al. 2010; Krauss 1979; Dawson 1959) and many other locations throughout the global tropics (Rejmánek and Richardson 2013; Mueller-Dombois and Fosberg 1998). Very dense Cocos canopies prevent easy recognition of individuals or the examination of tree spacing, necessitating a combined spectral and textural method implemented with high-resolution data.

4.2. Validation

A sample of 496 points was verified in the field and used to cross-validate the feature-selected classification of Palmyra Atoll. Cross-validation found *Scaevola sericea* shrubs to have the lowest user's accuracy at 88.7%, but the rest of the user's accuracies determined by cross-validation were all very high (>97.9%), and producer's accuracies for all classes exceeded 95%. While the OOB-based confusion matrix determined native forest to be the least accurately-modelled class by both accuracy metrics, cross-validation determined both accuracy metrics to be higher and more similar to the average accuracies across classes. Importantly, Cocos pixels were classified with 98.4% user's and producer's accuracies, indicating the model is extremely effective at classifying its primary target of interest. The generally high accuracies produced by the RF model may partially be a consequence of the small number of vegetation classes in our study site, as well as potential biases in our validation sampling strategy.

Our validation sampling strategy – although beginning with a simple random sample – only included points where land cover was deemed relatively homogenous for about 10 m in any direction. This approach was chosen as a way to compensate for the inaccuracy of our handheld GPS unit under the dense forest canopy: as the GPS unit's positional uncertainty potentially exceeded the size of both the WorldView-2 pixels (0.5 m) and the GLCM window (8.5 m), our very conservative sampling strategy ensured that the validation pixel on the image actually represented the land cover we observed on the ground. However, validation restricted to homogenous points has also been documented to produce overly-optimistic accuracy estimates in land cover studies (Stehman 2009; Hammond and Verbyla 1996). While this trade-off adds some uncertainty to our cross-validated accuracy estimates, the OOB accuracy estimates produced by the RF algorithm directly from the training dataset were very similar to the cross-validated accuracies: overall OOB accuracy was 95.4% OOB while cross-validated accuracy was 97.0% (see Table 3). Producer's and user's accuracies generated for each class by the two validation approaches differed on average by only 1.47% and 0.45%, respectively, with the greatest difference occurring in user's accuracy for native forest (5.90%).

The closeness of the OOB and cross-validated accuracies is significant because the 800 training points on which the OOB accuracies were based included many points within 10 m of class boundaries, i.e. in areas of non-homogenous land cover. Because these points were selected directly from the image, we did not have to account for the accuracy of the handheld GPS. OOB estimates of accuracy are also generally very close (or even slightly pessimistic) approximations of true classification accuracy (Janitza and Hornung 2018; Breiman 1996), lending further confidence to the cross-validated

accuracy estimates. One previous examination of validation bias with RF classifiers did find the same optimistic effect on the order of 10%, but notes that it drew validation points from a spatial subset spanning only 17% of the entire study region and differing from the broader region in terms of class distribution (Zhen et al. 2013). While Zhen et al. (2013) did not examine OOB errors, our seemingly reduced validation bias could be due to the much greater coverage of our validation points (>90% of the atoll's land area) and the representative distribution of said points across the four classes (see Table 3 and A1).

In general, class edges appear to be captured well by the classification (see Figure 7), and individual trees are often correctly classified even when surrounded by different land cover classes, indicating our GLCM calculation window is sufficiently small to preserve inter-class variability at the spatial scale of tree canopies. However, class edges are frequently a few pixels offset from their true locations (see Figure 7), indicating the 17-by-17 pixel GLCM window and 5-by-5 modal filter likely caused some minor loss of information. But on the whole, these inaccuracies are small, and larger GLCM windows appear to degrade overall class edge sensitivity. Many misclassifications of native trees as coconut palms occur at points where the native tree canopies are small or otherwise patchy, which most likely misled the RF model by appearing texturally similar to *Cocos* canopies. Large shadowed gaps between coconut palm crowns are also sometimes misclassified as native forest canopy, most likely because of the homogeneous texture of the shadowed area.

4.3. Feature selection

Interestingly, the feature-selected RF model showed no quantifiable improvement in OOB errors over the sixteen-feature model (see Figure 6). Overall OOB error is nearly the same (4.6% versus 4.5% for the sixteen-feature model) and the most accurately-classified vegetation types are the same for both (in order of decreasing accuracy: *Cocos* canopy, non-vegetated surface, *Scaevola* shrub, and native forest). This finding may indicate that for a mapping effort with so few classes, the feature selection effort is largely unnecessary. However, visual inspection of each classification product suggests that the feature-selected model is slightly more effective at mapping class boundaries and standalone trees.

4.4. Forest mapping results

Palmyra Atoll's vegetation was manually mapped in 2005 (Wegmann 2005; reproduced in 2009; Lafferty et al. 2010). This map illustrates the dominant tree types across the atoll's forests, but not to the scale of smaller stands or individual tree crowns. While the 2005 map and our remote sensing effort cannot be compared directly due to differences in methodology, the total extent of *Cocos*-dominated forest was estimated by (Wegmann 2005) as 0.92 km², fairly similar to the 1.00 km² value derived from this study. Total area of native forest, plus *Scaevola sericea* and *Terminalia catappa*, was estimated at 1.09 km² in 2005, while the total areas of *Scaevola* and native forest add up to 0.98 km² in this classification. Wegmann (2009) also uses nearest-neighbour density estimates to calculate a total of 52,992 ($\pm 3,864$) coconut palms taller than 2 m across the atoll as of 2005. Extrapolating this value to the slightly larger area of *Cocos* forest found by the present

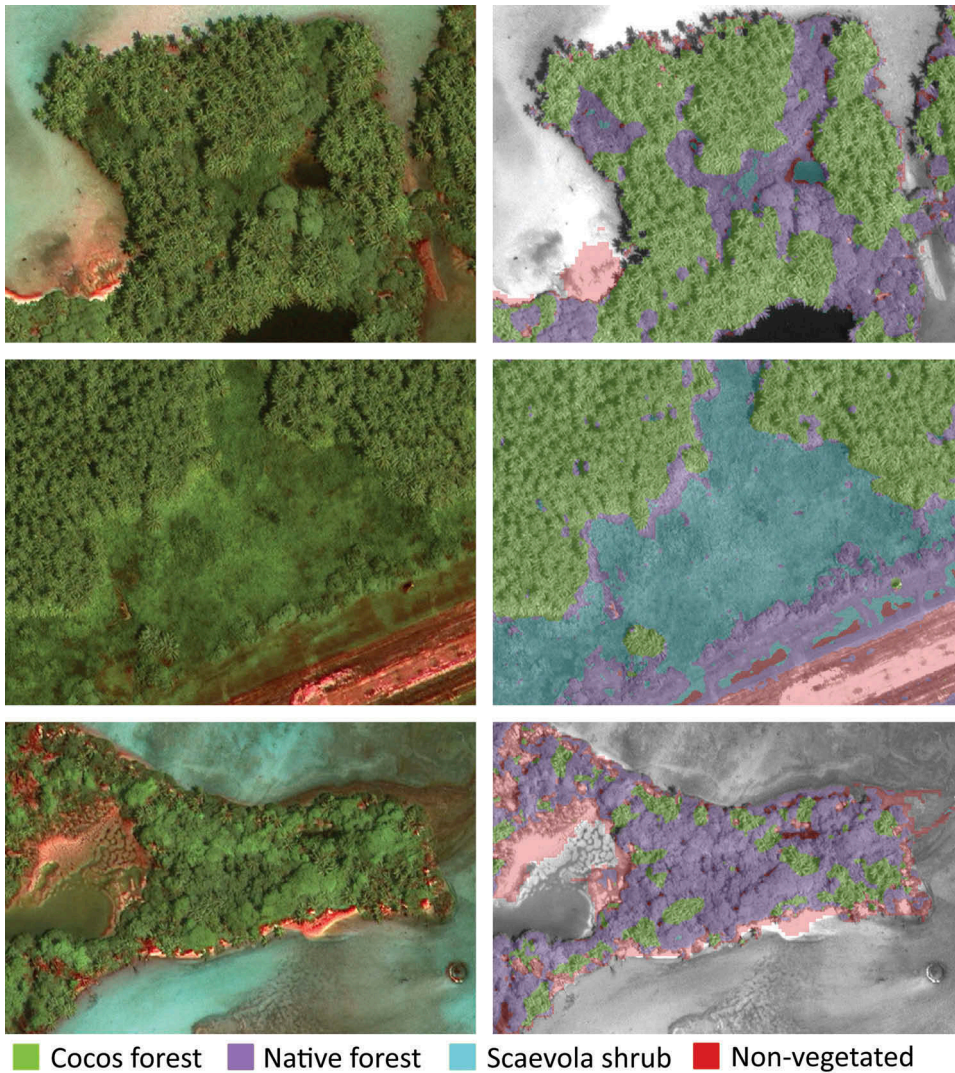


Figure 7. Left column: sections of Palmyra Atoll as seen in the pansharpened WV-2 image. Right column: the classification overlaid on top of the WV-2 image’s panspectral band (see legend at bottom). Top row: a section of Paradise Island (the atoll’s large southern islet) showing distinct Cocos-native forest edges; note the pond misclassified as *Scaevola* shrub. Middle row: a section of Cooper Island (the atoll’s large northern islet) showing a *Scaevola* thicket, the airstrip, and the edges of a Cocos forest. Bottom row: a section of native tree-dominated Eastern Island (the atoll’s north-eastern islet) showing the classification’s ability to pick out individual coconut palm trees. However, some of the spots classified as Cocos stands are false positives. Satellite images courtesy of the DigitalGlobe Foundation.

study yields an updated total of 57,600 ($\pm 4,200$) coconut palms, although this estimate does not account for any changes in Cocos density over the intervening decade.

The results of our classification show that most of Palmyra’s coconut palms occur on the larger portions of the atoll ring: Kaula Island (see [Figure A1](#)) has the highest proportion of land covered by Cocos (75.67%), and Holei and Paradise Islands

(connected to Kaula via narrow isthmuses) are also among the highest in the atoll (50.90% and 62.43%, respectively; see Appendix A). While Cooper Island, the largest in the atoll, is only 33.70% covered by *Cocos*, much of the island's land mass is protected from invasion by the maintenance of Palmyra's airstrip and field station. Strawn and Aviation Islands, linked to Cooper in similar fashion, have very high *Cocos* coverages at 59.39% and 74.43%. Meanwhile, sizeable islets like Sand and Eastern Islands are only 12.26% and 19.68% covered by *Cocos* canopy.

4.5. Future applications

We built our training dataset in a completely remote fashion to demonstrate the possibility that coconut palms could be classified on tropical islands with great accuracy without necessarily visiting the islands to collect ground-validated points, although prior knowledge of Palmyra's vegetation types informed the creation of the training dataset. As there are over 200 coral atoll islands like Palmyra across the Pacific and Indian oceans (Goldberg 2016) – not to mention larger volcanic islands – the challenges of visiting these isolated environments would quickly multiply if the spread of *Cocos* were to be assessed across the tropics. As verified by our ground-validated dataset, the 800 training points acquired only by inspecting remote imagery of Palmyra Atoll were able to produce accurate forest classifications and estimates of *Cocos* extent.

It is worth noting that Palmyra Atoll's environment offers a simple set of distinct vegetation types that undoubtedly contributed to the high classification accuracy obtained by the present study. While atoll and island ecosystems often do contain similar low-diversity assemblages of plant species, many other islands feature permanent human populations, elevated topographies, different climates, etc. All of these traits would likely contribute new land cover types that would need to be addressed before the methodologies described here could produce similarly high accuracies, and such high accuracies may not be achievable with a greater number of classes. For these reasons, wider attempts to remotely map *Cocos* and other island vegetation would need to consider the unique context of each island system when designing the training process. Beyond those considerations, researchers would be faced with another trade-off: spend the time and resources to re-train their algorithm for each island (or group of similar islands within the same image), or attempt to obtain surface reflectance values accurate enough to be applied wholesale to many islands at once – perhaps feasible with modern atmospheric correction techniques, but still a difficult path forward in the wet tropics (Cross et al. 2018; Song et al. 2001).

Ultimately, while the classifier's vegetation classes may need to be altered to suit the vegetation types of individual atolls or island groups, our approach's ability to detect unmanaged *Cocos* forests should remain strong in most locations with imagery suitable for the present study's combined spectral and textural methodology. Even considering islands with much greater diversities of vegetation cover, the unique morphological traits of *Cocos* canopies that proved easily detectable by GLCM feature extraction will still be present. With the increasing availability of very high resolution satellite imagery at affordable prices and the advent of machine learning models with effective built-in accuracy assessments, we suggest that the extent of *Cocos* forest could be estimated

over large ranges with remotely-acquired data, although firsthand or general knowledge of a given island's vegetation would certainly help inform the training process.

5. Conclusions

This study successfully demonstrates how a combination of several remote sensing methods and very high resolution satellite imagery can effectively assess an important and unquantified environmental problem. GLCM textural feature extraction is shown to be a highly effective supplement to standard multispectral remote sensing for differentiating between *Cocos* and broadleaf forests in an island environment. The random forest (RF) classifier also demonstrates its ability to produce a highly accurate classification in this system using very high resolution WorldView-2 data. Due to the great textural differences between *Cocos* and broadleaf canopies, tropical island forests turn out to be a model system for applying a joint spectral and textural classification approach, and an overall cross-validated accuracy of 97.0% is achieved for this simple four-class classification. *Cocos* classification accuracy increases from 79.0% to 98.0% when adding the eight GLCM textural features to the eight WV-2 spectral bands.

Given the great ecological impacts of *Pisonia* forest conversion to *Cocos* monocultures on atoll and island environments (Young et al. 2017; McCauley et al. 2012; Young et al. 2010), as well as *Pisonia*'s decline across the Pacific basin as a result of coconut palm agriculture (Krauss et al. 2015; Handler et al. 2007; Mueller-Dombois and Fosberg 1998; Walker 1991), the ability to remotely assess the forest composition of tropical islands is a critical next step in evaluating the health of these relatively inaccessible ecosystems. This study has demonstrated the viability of spectral and textural analysis by a machine learning algorithm (RF) for precisely mapping *Cocos* using the very high resolution imagery that is increasingly available to researchers, overcoming both the salt-and-pepper effect and the spectral similarity of *Cocos* trees to other island vegetation that has hampered previous research efforts (e.g. Lelong et al. 2004). In addition, the study tests the effectiveness of remotely-acquired training data for growing the RF model – an important factor for expanding future studies' scopes to a greater number of islands, given the abundance of isolated islands across the global tropics. Using variants of this approach that consider the unique environmental context of each island and adjust the classification scheme accordingly, future studies may examine coconut palm proliferation in other island groups or even across large swaths of Earth's oceans. While expanding the study area to such a vast region would surely raise many methodological questions, the process outlined in this study should retain its ability to accurately recognize *Cocos* canopies in a wide range of locations. Such broad-scale assessments could guide efforts to establish conservation areas in key areas of native forest, inform *Cocos* removal projects, and help build datasets to understand ecological dynamics in the understudied tropical island system. To these ends, the entirety of this study's analysis was conducted on free, open-source software products, increasing the accessibility of this study's methodology.

Acknowledgments

We thank the US Fish and Wildlife Service, The Nature Conservancy, and the Palmyra Atoll Research Consortium (PARC) for logistical and research support. WorldView-2 imagery was provided by the DigitalGlobe Foundation. This is PARC contribution #146.

Disclosure statement

No potential conflict of interest was reported by the authors.

Funding

This work was supported by the Stanford University Human Centered Artificial Intelligence Initiative, a National Geographic Society Early Career Grant, grants from the Environmental Venture Projects (EVP) and Mentoring Undergraduates in Interdisciplinary Research (MUIR) programs of the Stanford Woods Institute for the Environment, and the US National Science Foundation's Graduate Research Fellowship Program (DGE-114747).

ORCID

Douglas J. McCauley  <http://orcid.org/0000-0002-8100-653X>

Giulio A. De Leo  <http://orcid.org/0000-0002-4186-3369>

Fiorenza Micheli  <http://orcid.org/0000-0002-6865-1438>

References

- Bartolucci, L. A., B. F. Robinson, and L. F. Silva. 1977. "Field Measurements of the Spectral Response of Natural Waters." *Photogrammetric Engineering and Remote Sensing* 43 (5): 595–598.
- Booth, D. J., and R. B. Oldfield. 1989. "A Comparison of Classification Algorithms in Terms of Speed and Accuracy after the Application of A Post-Classification Modal Filter." *International Journal of Remote Sensing* 10 (7): 1271–1276. doi:10.1080/01431168908903965.
- Boulesteix, A. L., S. Janitzka, J. Kruppa, and I. R. König. 2012. "Overview of Random Forest Methodology and Practical Guidance with Emphasis on Computational Biology and Bioinformatics." *Wiley Interdisciplinary Reviews: Data Mining and Knowledge Discovery* 2 (6): 493–507. doi:10.1002/widm.1072.
- Breiman, L. 1996. *Out-of-Bag Estimation*. Berkeley, CA: University of California Berkeley. <https://www.stat.berkeley.edu/~breiman/OOBestimation.pdf>
- Breiman, L. 2001. "Random Forests." *Machine Learning* 45 (1): 5–32. doi:10.1023/A:1010933404324.
- Bricher, P. K., A. Lucieer, J. Shaw, A. Terauds, and D. M. Bergstrom. 2013. "Mapping Sub-Antarctic Cushion Plants Using Random Forests to Combine Very High Resolution Satellite Imagery and Terrain Modelling." *PLOS ONE* 8 (8): 1–15. doi:10.1371/journal.pone.0072093.
- Briggs, A. A., H. S. Young, D. J. McCauley, S. A. Hathaway, R. Dirzo, and R. N. Fisher. 2012. "Effects of Spatial Subsidies and Habitat Structure on the Foraging Ecology and Size of Geckos." *PLOS ONE* 7 (8). doi:10.1371/journal.pone.0041364.
- Carlson, K. M., L. M. Curran, G. P. Asner, A. M. Pittman, S. N. Trigg, and J. M. Adeney. 2013. "Carbon Emissions from Forest Conversion by Kalimantan Oil Palm Plantations." *Nature Climate Change* 3 (3): 283–287. doi:10.1038/nclimate1702.
- Chen, C., A. Liaw, and L. Breiman. 2004. *Using Random Forest to Learn Imbalanced Data*. Berkeley, CA: University of California Berkeley. <https://statistics.berkeley.edu/sites/default/files/tech-reports/666.pdf>
- Clausi, D. A. 2002. "An Analysis of Co-Occurrence Texture Statistics as a Function of Grey Level Quantization." *Canadian Journal of Remote Sensing* 28 (1): 45–62. doi:10.5589/m02-004.
- Collen, J. D., D. W. Garton, and J. P. A. Gardner. 2009. "Shoreline Changes and Sediment Redistribution at Palmyra Atoll (Equatorial Pacific Ocean): 1874–Present." *Journal of Coastal Research* 25 (3): 711–722. doi:10.2112/08-1007.1.
- Cross, M. D., T. A. Scambos, F. Pacifici, and W. E. Marshall. 2018. "Validating the Use of Metre-Scale Multi-Spectral Satellite Image Data for Identifying Tropical Forest Tree Species." *International Journal of Remote Sensing* 39 (11): 3723–3752. doi:10.1080/01431161.2018.1448482.

- Cutler, D. R., T. C. Edwards, K. H. Jr., B. A. Cutler, K. T. Hess, J. Gibson, and J. J. Lawler. 2007. "Random Forests for Classification in Ecology." *Ecology* 88 (11): 2783–2792. doi:10.1890/07-0539.1.
- Dawson, E. Y. 1959. "Changes in Palmyra Atoll and Its Vegetation through the Activities of Man, 1913-1958." *Pacific Naturalist* 1 (2): 1–51.
- Evans, J. S., and S. A. Cushman. 2009. "Gradient Modeling of Conifer Species Using Random Forests." *Landscape Ecology* 24 (5): 673–683. doi:10.1007/s10980-009-9341-0.
- Fine, P. V. A. 2002. "The Invasibility of Tropical Forests by Exotic Plants." *Journal of Tropical Ecology* 18 (05): 687–705. doi:10.1017/S0266467402002456.
- Fordham, D. A., and B. W. Brook. 2010. "Why Tropical Island Endemics are Acutely Susceptible to Global Change." *Biodiversity and Conservation* 19 (2): 329–342. doi:10.1007/s10531-008-9529-7.
- Fosberg, F. R. 1957. "Description and Occurrence of Atoll Phosphate Rock in Micronesia." *American Journal of Science* 255: 584–592. doi:10.2475/ajs.255.8.584.
- Genuer, R., J. M. Poggi, and C. Tuleau-Malot. 2010. "Variable Selection Using Random Forests." *Pattern Recognition Letters* 31 (14): 2225–2236. doi:10.1016/j.patrec.2010.03.014.
- Goldberg, W. M. 2016. "Atolls of the World: Revisiting the Original Checklist." *Atoll Research Bulletin* 610: 1–47. doi:10.5479/si.0077-5630.610.
- Gordon, H. R., and M. Wang. 1992. "Surface-Roughness Considerations for Atmospheric Correction of Ocean Color Sensors. II: Error in the Retrieved Water-Leaving Radiance." *Applied Optics* 31 (21): 4261–4267. doi:10.1364/AO.31.004261.
- Gregorutti, B., B. Michel, and P. Saint-Pierre. 2017. "Correlation and Variable Importance in Random Forests." *Statistics and Computing* 27 (3): 659–678. doi:10.1007/s11222-016-9646-1.
- Hall-Beyer, M. 2017a. "Practical Guidelines for Choosing GLCM Textures to Use in Landscape Classification Tasks over a Range of Moderate Spatial Scales." *International Journal of Remote Sensing* 38 (5): 1312–1338. doi:10.1080/01431161.2016.1278314.
- Hall-Beyer, M. 2017b. *GLCM Texture: A Tutorial. Version 3.0*. Calgary, Alberta: University of Calgary. doi:10.11575/PRISM/33280.
- Hammond, T. O., and D. L. Verbyla. 1996. "Optimistic Bias in Classification Accuracy Assessment." *International Journal of Remote Sensing* 17 (6): 1261–1266. doi:10.1080/01431169608949085.
- Han, H., X. Guo, and H. Yu. 2016. "Variable Selection Using Mean Decrease Accuracy and Mean Decrease Gini Based on Random Forest." In 7th IEEE International Conference on Software Engineering and Service Science (ICSESS), 219–224. Beijing, China: IEEE. doi:10.1109/ICSESS.2016.7883053.
- Handler, A. T., D. S. Gruner, W. P. Haines, M. W. Lange, and K. Y. Kaneshiro. 2007. "Arthropod Surveys on Palmyra Atoll, Line Islands, and Insights into the Decline of the Native Tree *Pisonia grandis* (Nyctaginaceae)." *Pacific Science* 61 (4): 485–502. doi:10.2984/1534-6188(2007)61[485:asopal]2.0.co;2.
- Hansen, M. C., P. V. Potapov, R. Moore, M. Hancher, S. A. Turubanova, A. Tyukavina, D. Thau, et al. 2013. "High-Resolution Global Maps of 21st-Century Forest Cover Change." *Science* 342 (6160): 850–853. doi:10.1126/science.1244693.
- Haralick, R. M., K. Shanmugan, and I. Dinstein. 1973. "Textural Features for Image Classification." *IEEE Transactions on Systems, Man and Cybernetics* 3 (6): 610–621. doi:10.1109/TSMC.1973.4309314.
- Hathaway, S. A., K. McEachern, and R. N. Fisher. 2011. *Terrestrial Forest Management Plan for Palmyra Atoll: U.S. Geological Survey Open-File Report 2011–1007*.
- Hijmans, R. J. 2017. *Raster: Geographic Data Analysis and Modeling. R Package Version 2.6-7*. <https://cran.r-project.org/package=raster>
- Huang, C., and G. Asner. 2009. "Applications of Remote Sensing to Alien Invasive Plant Studies." *Sensors* 9 (6): 4869–4889. doi:10.3390/s90604869.
- Huang, X., X. Liu, and L. Zhang. 2014. "A Multichannel Gray Level Co-Occurrence Matrix for Multi/Hyperspectral Image Texture Representation." *Remote Sensing* 6 (9): 8424–8445. doi:10.3390/rs6098424.
- Immitzer, M., C. Atzberger, and T. Koukal. 2012. "Tree Species Classification with Random Forest Using Very High Spatial Resolution 8-Band WorldView-2 Satellite Data." *Remote Sensing* 4 (9): 2661–2693. doi:10.3390/rs4092661.

- Irons, J. R., and G. W. Petersen. 1981. "Texture Transforms of Remote Sensing Data." *Remote Sensing of Environment* 11: 359–370. doi:10.1016/0034-4257(81)90033-X.
- Janitzka, S., and R. Hornung. 2018. "On the Overestimation of Random Forest's out-Of-Bag Error." *PLOS ONE* 13. doi:10.1371/journal.pone.0201904.
- Kaszta, Z., R. Van De Kerchove, A. Ramoelo, M. A. Cho, S. Madonsela, R. Mathieu, and E. Wolff. 2016. "Seasonal Separation of African Savanna Components Using WorldView-2 Imagery: A Comparison of Pixeland Object-Based Approaches and Selected Classification Algorithms." *Remote Sensing* 8 (9): 763. doi:10.3390/rs8090763.
- Kepler, A. K., and C. B. Kepler. 1994. "The Natural History of Caroline Atoll, Southern Line Islands: Part I. History, Physiography, Botany, and Isle Descriptions." *Atoll Research Bulletin* 397: 1–225. doi:10.5479/si.00775630.397.1.
- Koh, L. P., J. Miettinen, S. C. Liaw, and J. Ghazoul. 2011. "Remotely Sensed Evidence of Tropical Peatland Conversion to Oil Palm." *Proceedings of the National Academy of Sciences* 108 (12): 5127–5132. doi:10.1073/pnas.1018776108.
- Komba Mayossa, P. C., G. C. d'Eeckenbrugge, F. Borne, S. Gadai, and G. Viennois. 2015. "Developing a Method to Map Coconut Agrosystems from High-Resolution Satellite Images." In 27th International Cartographic Conference, 16th General Assembly. Rio de Janeiro, Brazil: International Cartographic Association. doi:10.13140/RG.2.1.4618.8244.
- Krauss, B. 1979. "Palmyra: It's a Pioneer Life at the Copra Plantation." *The Honolulu Advertiser*, September 17.
- Krauss, K. W., J. A. Duberstein, N. Cormier, H. S. Young, and S. A. Hathaway. 2015. "Proximity to Encroaching Coconut Palm Limits Native Forest Water Use and Persistence on a Pacific Atoll." *Ecohydrology* 8: 1514–1524. doi:10.1002/eco.1601.
- Lafferty, K. D., S. A. Hathaway, A. S. Wegmann, F. S. Shipley, A. R. Backlin, J. Helm, and R. N. Fisher. 2010. "Stomach Nematodes (*Mastophorus Muris*) in Rats (*Rattus Rattus*) are Associated with Coconut (*Cocos Nucifera*) Habitat at Palmyra Atoll." *Journal of Parasitology* 96 (1): 16–20. doi:10.1645/GE-2180.1.
- Le Louarn, M., P. Clergeau, E. Briche, and M. Deschamps-Cottin. 2017. "'Kill Two Birds with One Stone': Urban Tree Species Classification Using Bi-Temporal Pléiades Images to Study Nesting Preferences of an Invasive Bird." *Remote Sensing* 9 (9): 916. doi:10.3390/rs9090916.
- Lee, J. S. H., S. Wich, A. Widayati, and L. P. Koh. 2016. "Detecting Industrial Oil Palm Plantations on Landsat Images with Google Earth Engine." *Remote Sensing Applications: Society and Environment* 4: 219–224. doi:10.1016/j.rsase.2016.11.003.
- Lelong, C. C. D., C. D. J. Lesponne, N. Lamanda, G. Lainé, and E. Malézieux. 2004. "Understanding the Spatial Structure of Agroforestry Systems Using Very High Resolution Remote Sensing: An Application to Coconut-Based Systems in Melanesia." In *1st World Congress of Agroforestry: Working Together for Sustainable Land Use Systems*, edited by P. K. R. Nair, 191. Gainesville, FL: University of Florida.
- Li, H., L. Jing, and Y. Tang. 2017. "Assessment of Pansharpening Methods Applied to WorldView-2 Imagery Fusion." *Sensors* 17 (1): 89. doi:10.3390/s17010089.
- Li, W., H. Fu, L. Yu, and A. Cracknell. 2016. "Deep Learning Based Oil Palm Tree Detection and Counting for High-Resolution Remote Sensing Images." *Remote Sensing* 9 (1): 22. doi:10.3390/rs9010022.
- Liaw, A., and M. Wiener. 2002. "Classification and Regression by RandomForest." *R News* 2: 18–22.
- Liu, D., and F. Xia. 2010. "Assessing Object-Based Classification: Advantages and Limitations." *Remote Sensing Letters* 1 (4): 187–194. doi:10.1080/01431161003743173.
- Ma, L., M. Li, X. Ma, L. Cheng, P. Du, and Y. Liu. 2017. "A Review of Supervised Object-Based Land-Cover Image Classification." *ISPRS Journal of Photogrammetry and Remote Sensing* 130: 277–293. doi:10.1016/j.isprsjprs.2017.06.001.
- Marceau, D. J., P. J. Howarth, J. M. Dubois, and D. J. Grattan. 1990. "Evaluation Of The Grey-Level Co-Occurrence Matrix Method For Land-Cover Classification Using Spot Imagery." *IEEE Transactions on Geoscience and Remote Sensing* 28 (4): 513–519. doi:10.1109/TGRS.1990.572937.
- McCauley, D. J., P. A. DeSalles, H. S. Young, R. B. Dunbar, R. Dirzo, M. M. Mills, and F. Micheli. 2012. "From Wing to Wing: The Persistence of Long Ecological Interaction Chains in Less-Disturbed Ecosystems." *Scientific Reports* 2: 409. doi:10.1038/srep00409.

- Millard, K., and M. Richardson. 2015. "On the Importance of Training Data Sample Selection in Random Forest Image Classification: A Case Study in Peatland Ecosystem Mapping." *Remote Sensing* 7 (7): 8489–8515. doi:10.3390/rs70708489.
- Mueller-Dombois, D., and F. R. Fosberg. 1998. "Vegetation of the Tropical Pacific Islands." In *Ecological Studies*, edited by M. M. Caldwell, G. Heldmaier, O. L. Lange, H. A. Mooney, E.-D. Schulze, and U. Sommer, 132. New York, NY: Springer. doi:10.1007/978-1-4419-8686-3.
- Murray, H., A. Lucieer, and R. Williams. 2010. "Texture-Based Classification of Sub-Antarctic Vegetation Communities on Heard Island." *International Journal of Applied Earth Observation and Geoinformation* 12 (3): 138–149. doi:10.1016/j.jag.2010.01.006.
- Myint, S. W., N. S.-N. Lam, and J. M. Tyler. 2004. "Wavelets for Urban Spatial Feature Discrimination: Comparisons with Fractal, Spatial Autocorrelation, and Spatial Co-Occurrence Approaches." *Photogrammetric Engineering and Remote Sensing* 70 (7): 803–812. doi:10.14358/PERS.70.7.803.
- Ozdemir, I., and A. Karnieli. 2011. "Predicting Forest Structural Parameters Using the Image Texture Derived from Worldview-2 Multispectral Imagery in a Dryland Forest, Israel." *International Journal of Applied Earth Observation and Geoinformation* 13 (5): 701–710. doi:10.1016/j.jag.2011.05.006.
- Pacifici, F. 2016. "Validation of the DigitalGlobe Surface Reflectance Product." In *International Geoscience and Remote Sensing Symposium (IGARSS) 2016*, 1973–1975. Beijing, China: IEEE. doi:10.1109/IGARSS.2016.7729508.
- Pacifici, F., M. Chini, and W. J. Emery. 2009. "A Neural Network Approach Using Multi-Scale Textural Metrics from Very High-Resolution Panchromatic Imagery for Urban Land-Use Classification." *Remote Sensing of Environment* 113 (6): 1276–1292. doi:10.1016/j.rse.2009.02.014.
- Pal, M. 2005. "Random Forest Classifier for Remote Sensing Classification." *International Journal of Remote Sensing* 26 (1): 217–222. doi:10.1080/01431160412331269698.
- Pal, M., and P. M. Mather. 2003. "An Assessment of the Effectiveness of Decision Tree Methods for Land Cover Classification." *Remote Sensing of Environment* 86 (4): 554–565. doi:10.1016/S0034-4257(03)00132-9.
- Pratomo, J., M. Kuffer, J. Martinez, and D. Kohli. 2017. "Coupling Uncertainties with Accuracy Assessment in Object-Based Slum Detections, Case Study: Jakarta, Indonesia." *Remote Sensing* 9 (11): 1164. doi:10.3390/rs9111164.
- Puissant, A., J. Hirscha, and C. Webera. 2005. "The Utility of Texture Analysis to Improve Per-Pixel Classification for High to Very High Spatial Resolution Imagery." *International Journal of Remote Sensing* 26 (4): 733–745. doi:10.1080/01431160512331316838.
- QGIS Development Team. 2009. "QGIS Geographic Information System." Open Source Geospatial Foundation (OSGeo). <http://qgis.osgeo.org>
- R Core Team. 2016. "R: A Language and Environment for Statistical Computing." Vienna, Austria: R Foundation for Statistical Computing. <https://www.r-project.org/>
- Rejmánek, M., and D. M. Richardson. 2013. "Trees and Shrubs as Invasive Alien Species - 2013 Update of the Global Database." *Diversity and Distributions* 19 (8): 1093–1094. doi:10.1111/ddi.12075.
- Rock, J. F. 1916. "Palmyra Island with a Description of Its Flora." *College of Hawaii Publications: Bulletin* 4: 1–53.
- Rodriguez-Galiano, V. F., M. Chica-Olmo, F. Abarca-Hernandez, P. M. Atkinson, and C. Jeganathan. 2012a. "Random Forest Classification of Mediterranean Land Cover Using Multi-Seasonal Imagery and Multi-Seasonal Texture." *Remote Sensing of Environment* 121: 93–107. doi:10.1016/j.rse.2011.12.003.
- Rodriguez-Galiano, V. F., B. Ghimire, J. Rogan, M. Chica-Olmo, and J. P. Rigol-Sanchez. 2012b. "An Assessment of the Effectiveness of a Random Forest Classifier for Land-Cover Classification." *ISPRS Journal of Photogrammetry and Remote Sensing* 67 (1): 93–104. doi:10.1016/j.isprsjprs.2011.11.002.
- Seddon, A. W. R., M. Macias-Fauria, P. R. Long, D. Benz, and K. J. Willis. 2016. "Sensitivity of Global Terrestrial Ecosystems to Climate Variability." *Nature* 531 (7593): 229–232. doi:10.1038/nature16986.
- Shiraishi, T., T. Motohka, R. B. Thapa, M. Watanabe, and M. Shimada. 2014. "Comparative Assessment of Supervised Classifiers for Land Use-Land Cover Classification in a Tropical

- Region Using Time-Series PALSAR Mosaic Data." *IEEE Journal of Selected Topics in Applied Earth Observations and Remote Sensing* 7 (4): 1186–1199. doi:10.1109/jstars.2014.2313572.
- Smith, M. J. 2015. "A Comparison of DG AComp, FLAASH and QUAC Atmospheric Compensation Algorithms Using WorldView-2 Imagery." M.S. diss., University of Colorado.
- Song, C., C. E. Woodcock, K. C. Seto, M. P. Lenney, and S. A. Macomber. 2001. "Classification and Change Detection Using Landsat TM Data: When and How to Correct Atmospheric Effects?" *Remote Sensing of Environment* 75 (2): 230–244. doi:10.1016/S0034-4257(00)00169-3.
- Srestasathien, P., and P. Rakwatin. 2014. "Oil Palm Tree Detection with High Resolution Multi-Spectral Satellite Imagery." *Remote Sensing* 6 (10): 9749–9774. doi:10.3390/rs6109749.
- Stehman, S. V. 2009. "Sampling Designs for Accuracy Assessment of Land Cover." *International Journal of Remote Sensing* 30 (20): 5243–5272. doi:10.1080/01431160903131000.
- Thenkabail, P. S., N. Stucky, B. W. Griscom, M. S. Ashton, J. Diels, B. Van der Meer, and E. Enclona. 2004. "Biomass Estimations and Carbon Stock Calculations in the Oil Palm Plantations of African Derived Savannas Using IKONOS Data." *International Journal of Remote Sensing* 10 (23): 5447–5472. doi:10.1080/01431160412331291279.
- Vergara, N. T., and P. K. R. Nair. 1985. "Agroforestry in the South Pacific Region — An Overview." *Agroforestry Systems* 3 (4): 363–379. doi:10.1007/bf00055718.
- Walker, T. A. 1991. "Pisonia Islands of the Great Barrier Reef. Part I. The Distribution, Abundance and Dispersal by Seabirds of *Pisonia Grandis*." *Atoll Research Bulletin* 348–354 (350): 1–23. doi:10.5479/si.00775630.350-1.1.
- Wang, T., H. Zhang, H. Lin, and C. Fang. 2016. "Textural-Spectral Feature-Based Species Classification of Mangroves in Mai Po Nature Reserve from Worldview-3 Imagery." *Remote Sensing* 8 (1): 24. doi:10.3390/rs8010024.
- Wegmann, A. S. 2005. *Palmyra Atoll National Wildlife Refuge Forest Type Map*. Honolulu, HI: U.S. Fish and Wildlife Service.
- Wegmann, A. S. 2009. "Limitations to Tree Seedling Recruitment at Palmyra Atoll." PhD diss., University of Hawai'i at Manoa.
- Wester, L. 1985. "Checklist of the Vascular Plants of the Northern Line Islands." *Atoll Research Bulletin* 287: 1–38. doi:10.5479/si.00775630.287.1.
- Young, H. S., D. J. McCauley, A. Pollock, and R. Dirzo. 2014. "Differential Plant Damage Due to Litterfall in Palm-Dominated Forest Stands in a Central Pacific Atoll." *Journal of Tropical Ecology* 30 (3): 231–236. doi:10.1017/S026646741400008X.
- Young, H. S., A. Miller-Ter Kuile, D. J. McCauley, and R. Dirzo. 2017. "Cascading Community and Ecosystem Consequences of Introduced Coconut Palms (*Cocos Nucifera*) in Tropical Islands." *Canadian Journal of Zoology* 95 (3): 139–148. doi:10.1139/cjz-2016-0107.
- Young, H. S., T. K. Raab, D. J. McCauley, A. A. Briggs, and R. Dirzo. 2010. "The Coconut Palm, *Cocos Nucifera*, Impacts Forest Composition and Soil Characteristics at Palmyra Atoll, Central Pacific." *Journal of Vegetation Science* 21 (6): 1058–1068. doi:10.1111/j.1654-1103.2010.01219.x.
- Yu, Q., P. Gong, N. Clinton, G. Biging, M. Kelly, and D. Schirokauer. 2006. "Object-Based Detailed Vegetation Classification with Airborne High Spatial Resolution Remote Sensing Imagery." *Photogrammetric Engineering and Remote Sensing* 72 (7): 799–811. doi:10.14358/pers.72.7.799.
- Zhen, Z., L. J. Quackenbush, S. V. Stehman, and L. Zhang. 2013. "Impact of Training and Validation Sample Selection on Classification Accuracy and Accuracy Assessment When Using Reference Polygons in Object-Based Classification." *International Journal of Remote Sensing* 34 (19): 6914–6930. doi:10.1080/01431161.2013.810822.
- Zvoleff, A. 2016. "GlcM: Calculate Textures from Grey-Level Co-Occurrence Matrices (Glcms)." R Package Version 1.6.1.. <https://cran.r-project.org/package=glcm>

Appendix A

Palmyra's islets are extremely variable in their sizes and vegetation types (see Figure A1). The north and south portions of Palmyra's largely-artificial rim (Collen, Garton, and Gardner 2009) feature very large amounts of *Cocos nucifera*-dominated forest, perhaps due to post-war planting

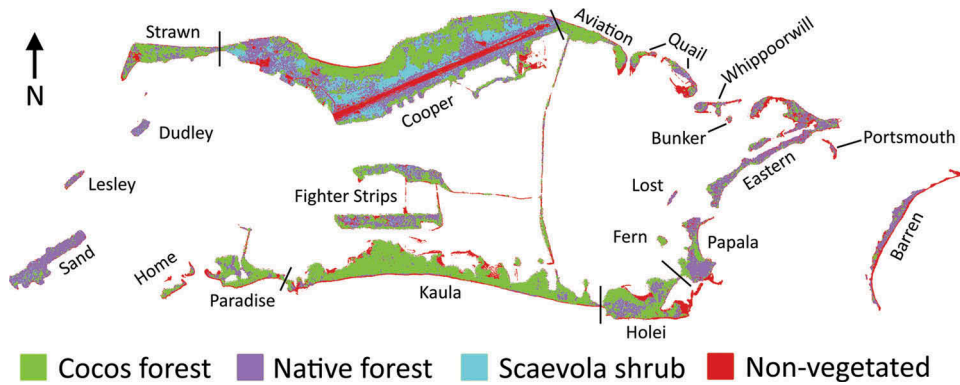


Figure A1. Classification map of Palmyra Atoll with islets labeled.

efforts targeting the largest islands (Hathaway, McEachern, and Fisher 2011; Krauss 1979). Meanwhile, several smaller islets constructed during the 1940s (Collen, Garton, and Gardner 2009) such as Sand, Lesley, and Dudley Islands feature mostly native broadleaf trees, and some of Palmyra's eastern rim (which existed in part before wartime dredging efforts) likewise features predominantly native forests. Cooper Island contains most of the atoll's *Scaevola sericea* shrubland, perhaps due to disturbances associated with the mile-long runway and small field station present on the island. Some islands referenced in earlier atoll maps have become joined to other land-masses (e.g. Bird Island to Holei Island), lost land area or split into fragments (e.g. Home Island, Quail Island), or almost completely disappeared (e.g. Dadu Island to the south of Barren Island) (see Collen, Garton, and Gardner 2009; Lafferty et al. 2010; Wegmann 2005).

Palmyra's islets vary greatly in Cocos coverage (see Table A1), with some major islets featuring as much as 75% Cocos-dominated forest canopy (Kaula) and others less than 20% (Eastern, Sand). The non-vegetated fraction of islets is much greater on some small islets, where sand banks surrounding the vegetated area are proportionally very large. Many islets in

Table A1. Land cover compositions of the islets of Palmyra, as designated in Figure A1. Islets are sorted by total land area.

Islet	% Cocos	% Native forest	% <i>Scaevola</i>	% Non-veg.	Total area (m ²)
Palmyra	42.31	33.40	8.23	16.07	2,365,387 ^a
Cooper	33.70	33.87	18.67	13.76	974,112
Kaula ^b	75.67	8.12	0.14	16.07	368,239
Holei ^c	50.90	30.72	1.22	17.15	151,174
Eastern	19.68	58.76	0.25	21.32	142,909
South Strip	42.81	43.00	2.30	11.90	93,777
Strawn	59.39	29.00	1.15	10.45	86,187
Paradise	62.43	21.18	0.65	15.74	85,529
Papala ^d	28.44	56.69	0.17	14.70	79,198
Sand	12.26	81.75	2.42	3.56	78,633
North Strip	49.45	39.18	4.33	7.04	68,983
Aviation	74.43	15.73	0.31	9.53	60,094
Barren ^e	9.34	47.79	0.21	42.66	55,447
Quail	25.98	31.82	0.87	41.33	41,849
Whippoorwill	18.80	47.86	0.01	33.32	17,282

(Continued)

Table A1. (Continued).

Islet	% <i>Cocos</i>	% Native forest	% <i>Scaevola</i>	% Non-veg.	Total area (m ²)
Home	37.57	17.04	0.00	45.39	15,315
Dudley	8.07	83.86	4.04	4.02	10,465
Lesley	13.37	69.46	0.00	17.17	8,012
Portsmouth	3.02	29.50	0.15	67.33	4,827
Fern	74.89	11.99	0.00	13.12	4,169
Lost	4.10	77.84	0.20	17.86	2,979
Bunker	19.76	38.35	0.00	41.89	1,867

^a Note that the total land area for Palmyra is greater than the sum of the following islet areas. This discrepancy is due to the exclusion of some sand banks and rocks classified as non-vegetated land by the RF classification, but not defined here as part of any of Palmyra's islets.

^b Kaula Island as described here is sometimes divided into Kaula, Marine, and Engineer Islands.

^c Holei Island as described here includes the two Bird Islands that were joined to Holei by shifting sand relatively recently.

^d Papala Island as described here is sometimes divided into Papala and Pelican Islands.

^e Barren Island as described here includes the small islands Garron and Dadu.

our classification reported very little *Scaevola sericea* presence – although *Scaevola* is considered common across the atoll, it is often covered by the canopies of larger *Tournefortia*, *Pisonia*, *Cocos*, or *Pandanus* trees, or on some islets restricted to narrow beach areas.